Article

Photoisomerization and Photodissociation of Aniline and 4-Methylpyridine

Chien-Ming Tseng, Yuri A. Dyakov, Cheng-Liang Huang, Alexander M. Mebel, Sheng Hsien Lin, Yuan T. Lee, and Chi-Kung Ni

J. Am. Chem. Soc., **2004**, 126 (28), 8760-8768• DOI: 10.1021/ja0483894 • Publication Date (Web): 22 June 2004

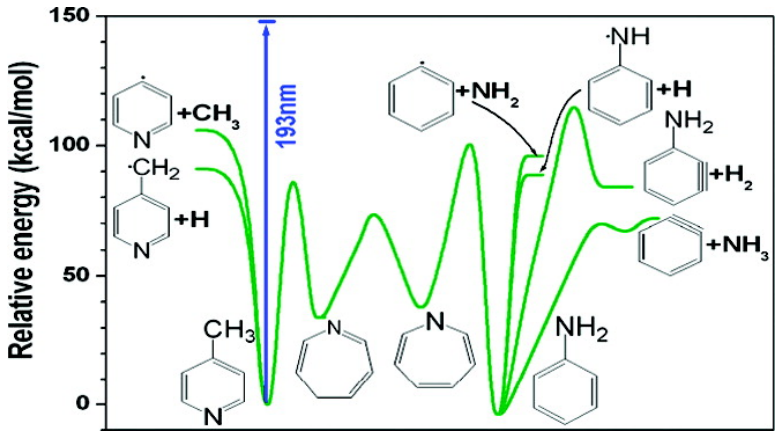

More About This Article

Additional resources and features associated with this article are available within the HTML version:

- Supporting Information
- Links to the 2 articles that cite this article, as of the time of this article download
- Access to high resolution figures
- Links to articles and content related to this article
- Copyright permission to reproduce figures and/or text from this article

View the Full Text HTML

Journal of the American Chemical Society is published by the American Chemical Society. 1155 Sixteenth Street N.W., Washington, DC 20036

J|A|C|S
ARTICLES
Published on Web 06/22/2004

Photoisomerization and Photodissociation of Aniline and 4-Methylpyridine

Chien-Ming Tseng,[†] Yuri A. Dyakov,[†] Cheng-Liang Huang,[†,‡] Alexander M. Mebel,[†,§] Sheng Hsien Lin,[†,||] Yuan T. Lee,[†,||] and Chi-Kung Ni*,[†]

Contribution from the Institute of Atomic and Molecular Sciences, Academia Sinica, P.O. Box 23−166, Taipei, Taiwan and Chemistry Department, National Taiwan University, Taipei, Taiwan

Received March 21, 2004; E-mail: ckni@po.iams.sinica.edu.tw

Abstract: Photoisomerization and photodissociation of aniline and 4-methylpyridine at 193 nm were studied separately using multimass ion imaging techniques. Photofragment translational energy distributions and dissociation rates were measured. Our results demonstrate that more than 23% of the ground electronic state aniline and 10% of 4-methylpyridine produced from the excitation by 193 nm photons after internal conversion isomerize to seven-membered ring isomers, followed by the H atom migration in the seven-membered ring, and then rearomatize to both methylpyridine and aniline prior to dissociation. The significance of this isomerization is that the carbon, nitrogen, and hydrogen atoms belonging to the alkyl or amino groups are involved in the exchange with those atoms in the aromatic ring during the isomerization.

I. Introduction

Today, aromatic photochemistry is a major area of study. The conspicuous feature that has emerged from the studies of aromatic photochemistry is that the photoexcitation of the benzene ring leads to a rich variety of reactions. The UV fluorescence quantum yields of aromatic molecules in the S_1 state decrease rapidly with the increase of photon energy.[1−5] For these molecules, the most important monomolecular processes after excitation to the S_1 state is photoisomerization with formation of the derivatives of fulvenes, benzvalenes, prismanes, as well as isomerization with a change of the alkyl substitute's position in the aromatic ring.[6−10] The generally accepted view is that photoisomerization of this kind proceeds by the intermediary formation of isomers such as benzvalene and prismane with their further rearomatization. It has been suggested that all isomerization processes of benzene and its alkyl derivatives can be described in terms of ring permutation.[11] The ring permutation has been observed in benzene and alkyl-substituted benzene in the condensed phase and in the gas phase after the excitation to the S_1 state.[6,12,13] The similar ring permutation were also used to describe the isomerization of nitrogen contained heterocyclic aromatic molecules.[14−16] Recently, different isomerization mechanism has been suggested, which involves the ring closure, followed by nitrogen migration around the sides of the cyclopehtenyl ring, and then rearomatization.[17−19] One important characteristic of both the ring permutation and ring closure mechanisms is that the carbon (or nitrogen) and hydrogen atoms belonging to the alkyl groups (or amino group) are *not* involved in the exchange with those atoms in the aromatic ring.

As the photon energy increases, the rate of internal conversion increases rapidly. Internal conversions of benzene and its derivatives are known to take place in subpicosecond time scale for the S_2 state.[20] Most of these molecules in the S_2 state undergo internal conversion to the ground electronic state and become highly vibrational excited, or "hot molecule". Since the energy of the S_2 state is much larger than the bond energy, dissociation is expected to occur. However, because of the sharing of internal

[†] Institute of Atomic and Molecular Sciences, Academia Sinica.
[‡] Present address: Department of Applied Chemistry, National Chiayi University, Chiayi, Taiwan.
[§] Present Address: Department of Chemistry and Biochemistry, Florida International University, Miami, FL 33199.
[||] Chemistry Department, National Taiwan University.

(1) Otis, C. E.; Knee, J. L.; Johnson, P. M. *J. Chem. Phys.* **1983**, *78*, 2091−2092.
(2) Nakashima, N.; Yoshihara, K. *J. Chem. Phys.* **1982**, *77*, 6040−6050.
(3) Sumitani, M.; Oconnor, D. V.; Takagi, Y.; Nakashima, N.; Kamogawa, K.; Udagawa, Y.; Yoshihara, K.; *Chem. Phys.* **1985**, *93*, 359−371.
(4) Duncan, M. A.; Dietz, T. G.; Liverman, M. G.; Smalley, R. E. *J. Phys. Chem.* **1981**, *85*, 7−9.
(5) Suto, M.; Wang, X.; Shan, J.; Lee, L. C. *J. Quant. Spectrosc. Radiat. Transfer*. **1992**, *48*, 79−89.
(6) Wilzbach, K. E.; Kaplan, L. *J. Am. Chem. Soc.* **1964**, *86*, 2307−2308.
(7) Burgstahler, A. W.; Chien, P. L. *J. Am. Chem. Soc.* **1964**, *86*, 2940−2941.
(8) Kaplan, L.; Wilzbach, K. E.; *J. Am. Chem. Soc.* **1967**, *89*, 1030−1031.
(9) Wilzbach, K. E.; Kaplan, L. *J. Am. Chem. Soc.* **1965**, *87*, 4004−4006.
(10) Den Besten, I. E.; Kaplan, L.; Wilzbach, K. E. *J. Am. Chem. Soc.* **1968**, *90*, 5868−5872.
(11) Bryce-Smith, D.; Gilbert, A. In *Rearrangement in Ground and Excited States*; De Mayo, P., Ed.; Academic Press: New York, 1980; Vol. 3.
(12) Jackson, A. H.; Kenner, G. W.; McGillvray, G.; Sach, G. S. *J. Am. Chem. Soc.* **1965**, *87*, 675−676.
(13) Wilzbach, K. E.; Harkness, A. L.; Kaplan, L. *J. Am. Chem. Soc.* **1968**, *90*, 1116−1118.
(14) Wilzbach, K. E.; Rausch, D. J. *J. Am. Chem. Soc.* **1970**, *92*, 2178−2179.
(15) Caplain, S.; Lablache-Combier, A. *Chem. Commun.* **1970**, 1247−1248.
(16) Johnson, D. W.; Austel, V.; Feld, R. S.; Lemal, D. M. *J. Am. Chem. Soc.* **1970**, *92*, 7505−7506.
(17) J. W. Pavlik, J. W.; Kebede, N.; Thompson, M.; Day, A. C.; Barltrop, J. A. *J. Am. Chem. Soc.* **1999**, *121*, 5666−5673.
(18) Pavlik, J. W.; Tongcharoensirikul, P.; Bird, N. P.; Day, A. C.; Barltrop, J. A. *J. Am. Chem. Soc.* **1994**, *116*, 2292−2300.
(19) MacLeod, P. J.; Pincock, A. L.; Pincock, J. A.; Thompson, K. A. *J. Am. Chem. Soc.* **1998**, *120*, 6443−6450.
(20) Radloff, W.; Freudenberg, Th.; Ritze, H. H.; Stert, V.; Noack, F.; Hertel, I. V. *Chem. Phys. Lett.* **1996**, *261*, 301−306.

10.1021/ja0483894 CCC: $27.50

energy among a large number of vibrational degrees of freedom in the hot molecules, the dissociation of a hot molecule is a rather slow process. For example, for a benzene molecule with the internal energy of 146 kcal/mol which is far exceeding the C−H bond dissociation energy of 110 kcal/mol, the average dissociation lifetime is as long as 10 μs.[21] One of the very interesting aspects of benzene and its derivatives is the fact that below the bond dissociation energy, there are many structural isomers and the activation energy for isomerization also lies below the bond dissociation energy. Consequently, isomerization processes are expected to take place before a molecule finds its way to dissociate.

More recently, we observed a small amount of CD_2H, CDH_2, and CH_3 and their heavy fragment partners, C_6H_4D, $C_6H_3D_2$, $C_6H_2D_3$, from the dissociation of isotope-labeled toluene, $C_6H_5CD_3$, after the excitation to the S_2 state.[22] It clearly indicates that direct C−H bond and C−C bond cleavages in the ground electronic state are not the only dissociation mechanism. Another dissociation channel must exist, which allows for the exchange of D atoms in the methyl group with H atoms in the aromatic ring prior to dissociation. In addition, the small amount of CH_3 resulting from $C_6H_5{}^{13}CH_3$ dissociation suggests that not only are hydrogen atoms involved in the scrambling, but also that carbon atoms in both the methyl group and the aromatic group are involved in the exchange. The result was interpreted as the isomerization from six-membered ring to seven-membered ring (cycloheptatriene), followed by H atom migration within seven-membered ring molecule, and then rearomatization prior to dissociation.[22] Similar isomerization was also observed in the photodissociation of xylene.[23] The significance of this isomerization is that it is totally different from the ring permutation, since the carbon atoms and hydrogen atoms belonging to the alkyl group are *not* involved in the exchange with those atoms in the aromatic ring during the ring permutation.

However, this particular isomerization in alkyl-substituted benzenes can only be observed using isotope-labeled compounds. For nonisotope-labeled molecules, the effect of this isomerization is equivalent to that of ring permutation. For example, the consequence of xylene through this isomerization is the exchange of relative alkyl group positions, which gives practically the same result as the ring permutation. On the other hand, if this isomerization is open for heterocyclic aromatic molecules, then it is not necessary to have isotope-labeled compounds and one can easily change the chemical function groups during the process. For instance, methylpyridine can be changed to aniline through this isomerization.

In this work, we extend the study to photoisomerization of aniline and 4-methylpyridine. The results suggest that the isomerization from six-membered ring to seven-membered ring after internal conversion also plays a very important role in nitrogen atom contained aromatic molecules. A comparison of 4-methylpyridine and aniline with potential energy from ab intito calculation and toluene has been made.

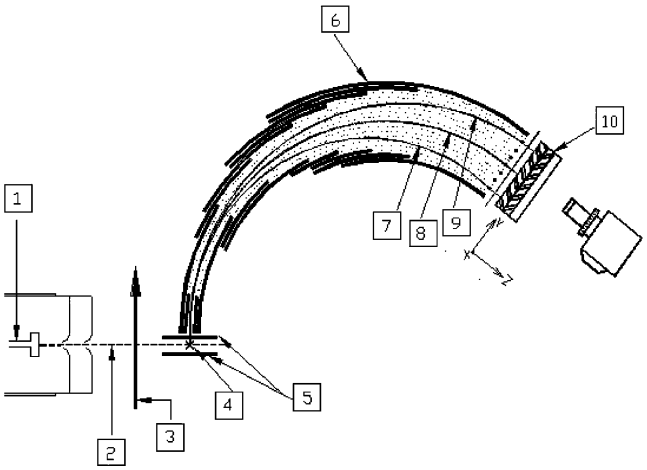

Figure 1. Schematic diagram of the multimass ion imaging detection system. (1) nozzle, (2) molecular beam, (3) photolysis laser beam, (4) VUV laser beam, (5) ion extraction plates, (6) mass spectrometer, (7),(8),(9) simulation trajectories of m/e = 16, 14, 12, (10) 2D ion detector.

II. Experiment

The experimental techniques have been described in detail in our previous reports on other aromatic molecules,[24,25] and only a brief description is given here. Aniline or 4-methylpyridine vapor was formed by flowing ultrapure He (or Ne) at pressures of 500 Torr through a reservoir filled with liquid sample at 20 °C. The aniline/He or 4-methylpyridine/He mixture was then expanded through a 500 μm pulsed nozzle at 50 °C to form a molecular beam. Molecules in the molecular beam were photodissociated by a 193 nm laser pulse. Due to the recoil velocity and center-of-mass velocity, the fragments were expanded to a larger sphere on their flight to the ionization region, and then ionized by a VUV laser pulse. The VUV wavelength we used was 118.2 nm. The distance and time delay between the VUV laser pulse and the photolysis laser pulse were set such that the VUV laser beam passed through the center-of-mass of the dissociation products, and generated a line segment of photofragment ions through the center-of-mass of the dissociation products by photoionization. The length of the segment was proportional to the fragment recoil velocity in the center-of-mass frame multiplied by the delay time between the photolysis and the ionization laser pulses. To separate the different masses within the ion segment, a pulsed electric field was used to extract the ions into a mass spectrometer after ionization. While the mass analysis was being executed in the mass spectrometer, the length of each fragment ion segment continued to expand in the original direction according to its recoil velocity. At the exit port of the mass spectrometer, a two-dimensional ion detector was used to detect the ion positions and intensity distribution. In this two-dimensional detector, one direction was the recoil velocity axis and the other was the mass axis. The identification of the dissociation products and the measurement of their translational energy distributions were therefore simultaneously obtained from the image. The schematic diagram of the experimental set up is shown in Figure 1.

The dissociation rates were obtained from the product growths or the decay of parent molecules with respect to the delay time between the pump and probe lasers using time-of-flight mass spectrometer. However, accurate measurement can be achieved only when the dissociation rate is fast enough before the parent molecules and fragments fly out of the detection region due to the molecular beam velocity and recoil velocity.

(21) Tsai, S. T.; Lin, C. K.; Lee, Y. T.; Ni, C. K. *J. Chem. Phys.* **2000**, *113*, 67−70.
(22) Lin, C. K.; Huang, C. L.; Jiang, J. C.; Chang, H.; Lin, S. H.; Lee, Y. T.; Ni, C. K. *J. Am. Chem. Soc*. **2002**, *124*, 4068−4075.
(23) Huang, C. L.; Jiang, J. C.; Lee, Y. T.; Ni, C. K. *J. Phys. Chem. A.* **2003**, *107*, 4019−4024.
(24) Tsai, S. T.; Lin, C. K.; Lee, Y. T.; Ni, C. K. *Rev. Sci. Instrum.* **2001**, *72*, 1963−1969.
(25) Tsai, S. T.; Huang, C. L.; Lee, Y. T.; Ni, C. K. *J. Chem. Phys.* **2001**, *115*, 2449−2455.

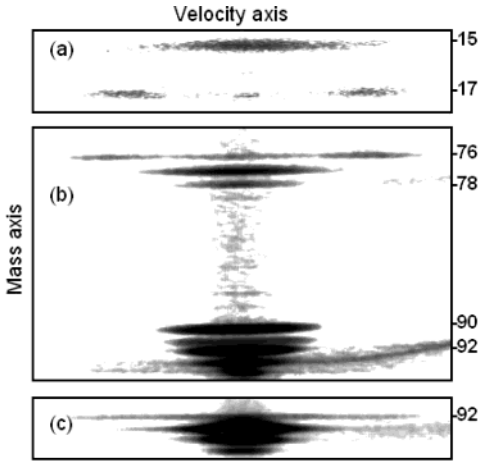

Figure 2. Photofragment ion images of aniline in three different mass regions. (a) $m/e = 15\sim17$, (b) $m/e = 75\sim94$, and (c) $91\sim95$. The pump and probe delay time between two laser pulses were 2.5, 15, and 83 μs, respectively. The delay time in (c) was very long such that the fragment $m/e = 91$ flight out of the detection region.

Aniline (99.8%), d_5-aniline (99%), and 4-methylpyridine (99%) were purchased from Acros Organics. d_3-4-methylpyridine (98%) was from Aldrich. These chemicals were used directly without further purification. The amounts of impurities were checked by both TOF mass spectrum and NMR spectroscopy. Mass spectrum shows that the total ion intensity of m/e values other than that of parent molecule is less than 1% in both aniline and 4-methylpyridine. In addition, NMR spectroscopy shows that no 4-methylpyridine can be detected in aniline, and no aniline can be detected in the 4-methylpyridine (less than 0.3% according to the S/N ratio of the spectrum).

III. Results

Aniline. Figure 2 shows the photofragment ion images of aniline. Fragments of $m/e = 92$, 91, 90, 78, 77, 76, 17, and 15 were observed. The study of photolysis laser power dependence in the region of $1.2\sim10$ mJ/cm^2 showed that $m/e = 90$ was due to the two photon dissociation and all the other fragments were from one-photon dissociation. Fragments resulted from multiphoton dissociation will not be discussed in this work.

Images of $m/e = 92$, 91, 77, and 76 represent four major dissociation channels of aniline, i.e., H, H_2, NH_2, and NH_3 eliminations, respectively. Some of the light fragment partners with ionization potentials lower than the VUV photon energy were observed, as presented in Figure 2a. In addition, the image intensity of $m/e = 78$ is 2.8 times larger than that of ^{13}C isotope of $m/e = 77$, indicating the existence of fragment C_5NH_4. It corresponds to the minor dissociation channel of CH_3 elimination. This channel can be further confirmed by the observation

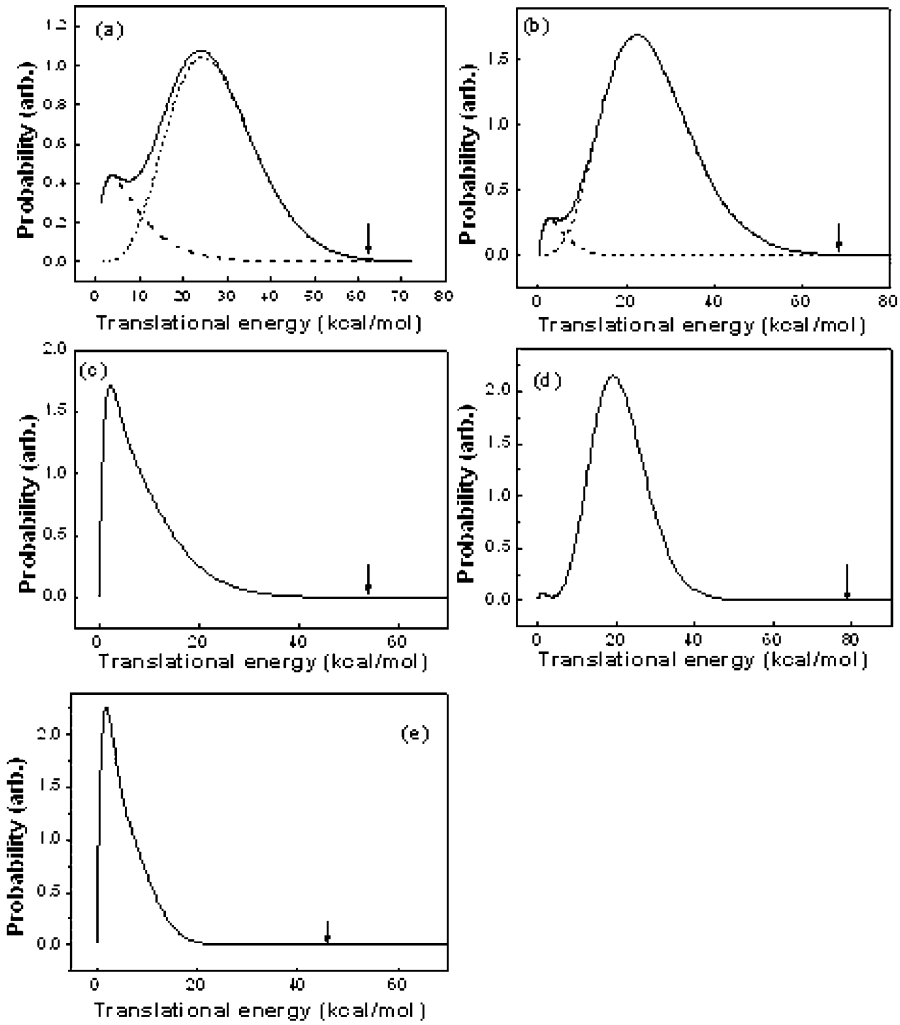

Figure 3. Photofragment translational energy distributions of (a) $C_6H_5NH_2 \rightarrow C_6H_5NH + H$, (b) $C_6H_5NH_2 \rightarrow C_6H_3NH_2 + H_2$, (c) $C_6H_5NH_2 \rightarrow C_6H_5 + NH_2$, (d) $C_6H_5NH_2 \rightarrow C_6H_4 + NH_3$, (e) $C_6H_5NH_2 \rightarrow C_5NH_4 + CH_3$. Arrows indicate the maximum available energies in each dissociation channel.

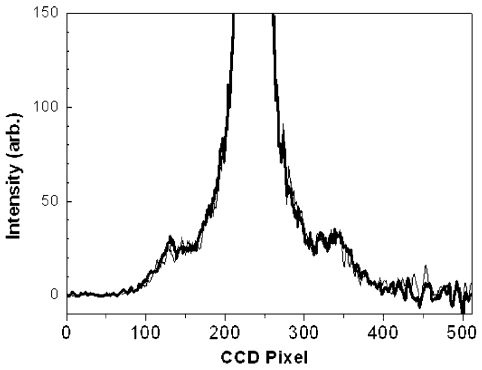

Figure 4. Image intensity profiles of $m/e = 92$ at the photolysis laser polarization parallel (thick solid line) and perpendicular (thin solid line) to the VUV laser beam.

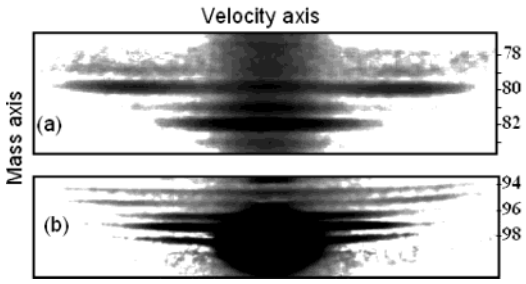

Figure 5. Photofragment ion images of d_5-aniline (a) $m/e = 78\sim83$ (b) $m/e = 94\sim100$.

of its light fragment partner CH_3, as shown in Figure 2a. The momentum matches between the heavy and light fragment partners also exclude the contribution from three-body dissociation, like the dissociation of clusters, or the contribution from cation dissociation. Some fragments corresponding to the ring-opening dissociation channel like $m/e = 66$, 54, 53, 52, 41, 40, and 39 were also observed. However, they were all very small and will not be discussed in this work.

Photofragment translational energy distributions obtained from the image are illustrated in Figure 3. Translation energy distribution of H atom elimination shows two components. The ratio between the fast and slow components is about 3:1. For the slow component, the average translational energy release is small and the probability of fragment translational energy distribution decreases monotonically with the increase of energy. These are the typical characteristics of the dissociation from hot molecules. On the other hand, the average released translational energy for the fast component is large, and the peak of the distribution is located at 24 kcal/mol. It must result from a repulsive state, or a state with a large exit barrier. Image intensity profiles of $m/e = 92$ at the photolysis laser polarization parallel and perpendicular to the VUV laser beam are shown in Figure 4. They have the same shape and intensity, indicating the isotropic fragment distribution of both the slow and fast H atom components.

Two-component translational energy distribution was also observed in H_2 elimination channel. The ratio between the fast and slow components is about 10:1. For the NH_3, CH_3, and NH_2 eliminations, however, there is only one component in the translational energy distribution. A dissociation rate of $(4.5 \pm 1) \times 10^6$ s^{-1} was obtained from the $m/e = 91$, 78, 77, and 76 product growths with respect to the delay time between pump and probe laser pulses. The same dissociation rate suggests the dissociation of these channels must occur in the same electronic state.

Isotope substituted d_5-aniline was also studied. The fragment ion images are shown in Figure 5. It shows that C_6D_4, corresponding to NH_2D elimination is the major products from the ammonia molecular elimination channel. However, small amount of fragments $m/e = 79$ and 78, corresponding to the NHD_2 and ND_3 elimination were also observed. For amino group elimination, NH_2 elimination is the dominant process, as it is shown at $m/e = 82$. But small amount of fragments corresponding to NHD and ND_2 elimination were also found. Although fragments of C_6D_3H, $C_6D_3H_2$, C_6D_4H, C_6D_5, corresponding to the eliminations of NH_2D, ND_2, NHD, and NH_2 have the same masses as those of $C_5ND_2H_2$, C_5ND_3H, and C_5ND_4, corresponding to the eliminations of CD_3, CD_2H, and CDH_2. However, the study of nonisotope labeled aniline suggests that the contribution from methyl group elimination is much smaller than that from ammonia and amino group elimination. In addition, the image intensity distribution of ammonia elimination is very different from that of amino group elimination. They can be separated from each other easily. Similar isotope substituted fragments were also observed in both H atom and H_2 elimination channels. In these channels, H atom, HD, and D_2 molecule eliminations are the major channels and D atom elimination is the minor channel. However, no H_2 elimination was observed. The observation of these fragments indicates the D atom and H atom exchange to some extent prior to dissociation.

The relative intensities of these isotope substituted fragments and their translational energy distributions are shown in Figure 6. Although the translation energy distribution of H atom elimination channel has two components, however, the distribution of D atom elimination channel has only one component, and it decreases monotonically with the increase of energy. It suggests that dissociation mechanisms of H atom and D atom elimination are different. For the analogous H_2, NH_2, and NH_3 elimination channels, the translational energy distributions of these isotope substituted fragments show very similar distributions to each other, indicating the similar dissociation mechanism.

4-Methylpyridine. 4-Methylpyridine shows very similar dissociation channels to those of aniline. However, fragment relative intensities are very different. Photofragment ion images from the photodissociation of 4-methylpyridine at 193 nm are shown in Figure 7. The study of photolysis laser power dependence in the region of $7\sim28$ mJ/cm^2 showed that $m/e = 90$ and $m/e = 91$ resulted from two photon absorption. Images of $m/e = 92$ and 78 have the largest intensities, they represent two major dissociation channels of 4-methylpyridine, i.e., $C_5NH_4CH_3 \rightarrow C_5NH_4CH_2 + H$, and $C_5NH_4CH_3 \rightarrow C_5NH_4 + CH_3$. It is interesting to note that images of $m/e = 77$and 76 with small intensities were observed. They correspond to the NH_2 and NH_3 eliminations. In addition, fragment ions with small intensities of $m/e = 66$, 54, 53, 52, 41, 40, and 39 were also observed. However, these signals are very small and they will not be discussed in this work.

The fragment translational energy distributions obtained from the ion image are presented in Figure 8. Compared to the

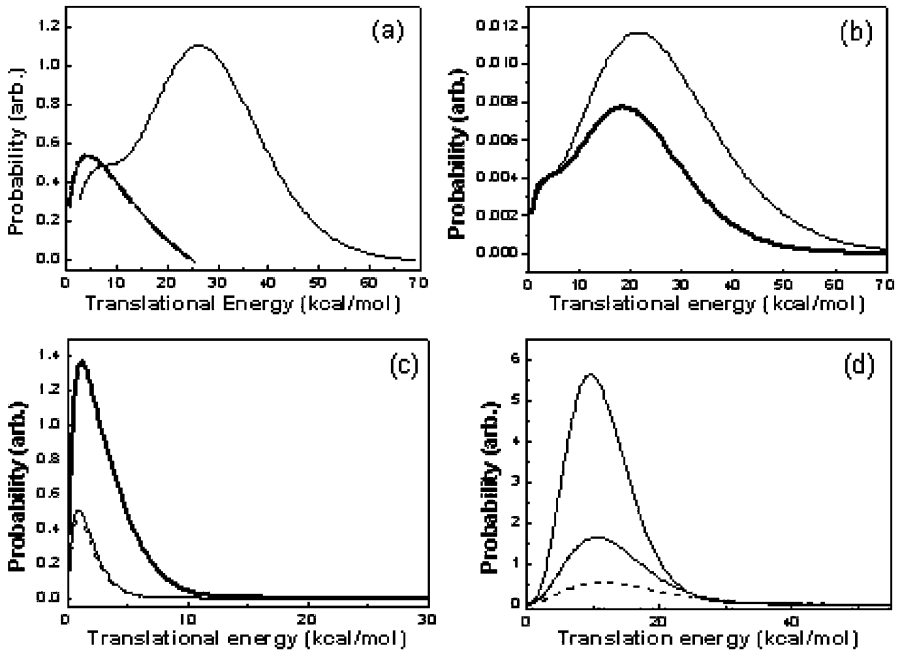

Figure 6. Photofragment translational energy distributions of d_5-aniline. (a) H (thin), D (thick) elimination. (b) HD (thin), D_2 (thick) elimination. (c) NH_2 (thick), NHD (dot), and ND_2 (thin) elimination. (d) NH_2D (thin), NHD_2 (thick), ND_3 (dot) elimination.

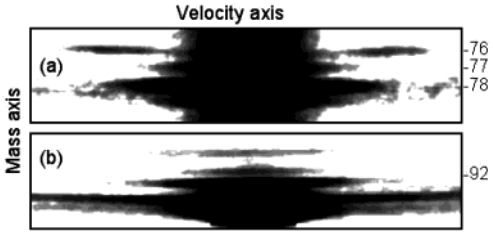

Figure 7. Photofragment ion images of 4-methylpyridine (a) $m/e = 75\sim80$.- (b) $m/e = 90\sim95$.

maximum available energies, the average released translation energies are all very small. They are only 5.4%, 7.1%, 19.4%, and 6.6% of the maximum available energies for H atom, CH_3, NH_3, and NH_2 elimination channels, respectively.

The similar dissociation channels were also observed in the photodissociation of d_3-4-methylpyridine. Photofragment images are shown in Figure 9. $m/e = 96$ was from parent molecule, $m/e = 95$ was from the contribution of H atom elimination as well as some incomplete isotope-labeled d_2-methylpyridine (5%), and $m/e = 94$ corresponded to the D atom elimination. Photofragments of $m/e = 78$, 79, 80, and 81 were mainly from C_5NH_4, C_5NH_3D, $C_5NH_2D_2$, and C_5NHD_3, as a result of CD_3, CHD_2, CH_2D, and CH_3 elimination. Since the ionization potential of NH_2 is larger than the VUV photon energy we used in this work, no amino radicals could be ionized. The relative branching ratios of CHD_2, CH_2D, and CH_3 elimination channels can be obtained directly from the intensity of light fragments in order to avoid the interference from ND_2, NHD, and NH_2 eliminations. Fragment ion intensity ratios were found to be CD_3:CD_2H:CDH_2:CH_3 = 91:3.6:4.5:0.9. Since the branching ratios of the analogues NH_2 and NH_3 elimination channels are very small, we did not intend to observe these channels for this isotope-labeled compound. The observation of various D atom substituted methyl radicals indicates that H and D atoms exchange before dissociation.

Dissociation rates of $(1.4 \pm 0.8) \times 10^6$ s^{-1} and $(1.8 \pm 0.5) \times 10^6$ s^{-1} were obtained from product growths with respect to the delay time between pump and probe laser pulses for $C_5NH_4CH_3$ and $C_5NH_4CD_3$, respectively. The dissociation rate of $C_5NH_4CD_3$ is only a little slower than that of $C_5NH_4CH_3$.

IV. Discussion

A. Dissociation and Isomerization Mechanisms. (a) 4-Methylpyridine. Previous studies of methylpyridine mainly focused on the excitation to the S_1 and S_2 states. The fluorescence quantum yield and intersystem crossing quantum yield decrease rapidly with the decrease of photon wavelength from 290 to 250 nm.[26] Fluorescence quantum yield changes from 10^{-4} at 290 nm to less than 2×10^{-6} at 250 nm and the quantum yield of intersystem crossing also drops from 0.8 to 0.04. Internal conversion to the ground electronic state becomes the dominant process. However, very little study has been done at the region of 193 nm. Since the methyl group is not an electronic chromophore in this region, UV absorption of 4-methylpyridine at 193 nm only correlates to the excitation of the electrons of the pyridyl ring. The excitation of the pyridyl ring results in an excited state, stable with respect to dissociation. Dissociation must occur either through the coupling of the stable and repulsive states, or after the internal conversion from an initial excited state to a lower electronic state. Since the dissociation in the ground state usually results in a limited release of kinetic energy due to the extensive energy randomization among vibrational degrees of freedom and has a slow dissociation rate, the observation of small kinetic energy release and slow dissociation rate suggest all of the 4-methylpyridine molecules relax to the ground electronic state through internal conversion prior to dissoci-

(26) Yamazaki, I.; Sushida, K.; Baba, H. *J. Chem. Phys.* **1979**, *71*, 381−387.

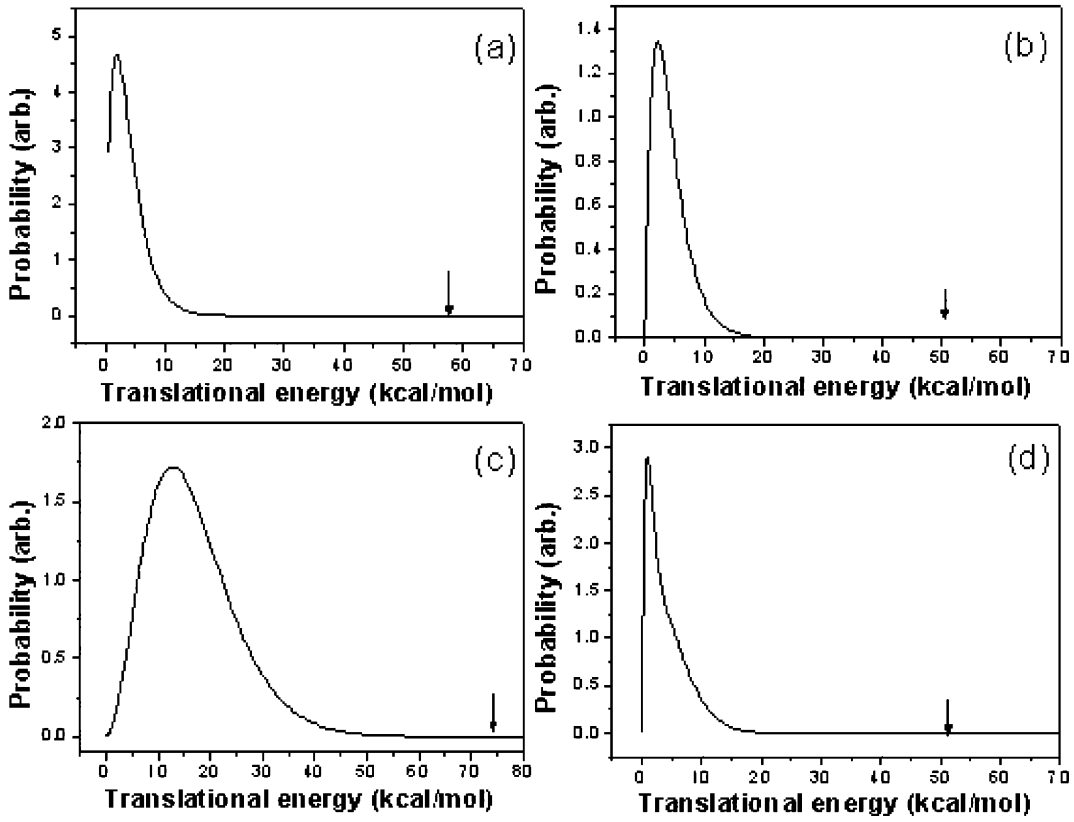

Figure 8. Photofragment translational energy distributions of reactions (a) $C_5NH_4CH_3 \rightarrow C_5NH_4CH_2 + H$ (b) $C_5NH_4CH_3 \rightarrow C_5NH_4 + CH_3$ (c) $C_5NH_4CH_3 \rightarrow C_6H_4 + NH_3$ (d) $C_5NH_4CH_3 \rightarrow C_6H_5 + NH_2$. Arrows indicate the maximum available energies in each dissociation channel.

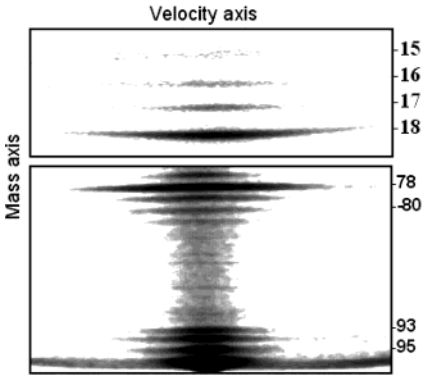

Figure 9. Photofragment ion images of d_3-picoline (a) $m/e = 15\sim18$ (b) $m/e = 77\sim96$.

ation. The results can be represented by the following reactions.

$$C_5NH_4CH_3 + h\nu_{193nm} \rightarrow C_5NH_4CH_3^* \text{ (excitation)} \quad (1)$$

$$C_5NH_4CH_3^* \rightarrow C_5NH_4CH_3^{\ddagger} \text{ (internal conversion to } S_0) \quad (2)$$

Here, $C_5NH_4CH_3^*$ represents 4-methylpyridine in the electronic excited states, and $C_5NH_4CH_{3\ddagger}$ represent 4-methylpyridine in the ground electronic state, respectively.

After internal conversion to the ground electronic state, 4-methylpyridine molecules could dissociate through various possible dissociation channels. Statistical transition-state theory has predicted that, given comparable pre-exponential factors for different bond fissions, the reaction pathway with the lowest energetic barrier should dominate the dissociation. Since the $C-CH_3$ and methyl C−H bond energies are relatively small compared to the other bond energies in the aromatic ring and these dissociation have no exit barrier because of the production of two radicals in the ground electronic state, H atom and CH_3 eliminations are expected to be the major dissociation channels. Indeed, they are the major channels observed in the experiment. These dissociation channels are described by the following reactions.

$$C_5NH_4CH_3^{\ddagger} \rightarrow C_5NH_4CH_2 + H$$
(direct dissociation after internal conversion) (3a)

$$C_5NH_4CH_3^{\ddagger} \rightarrow C_5NH_4 + CH_3$$
(direct dissociation after internal conversion) (3b)

However, the observation of C_6H_5 shows that a small fraction of 4-methylpyridine molecules go through a complicated isomerization prior to dissociation. To produce fragment C_6H_5 and NH_2 from 4-methylpyridine, H atoms in the molecule must migrate until nitrogen atom gathers two H atoms and then C−N bond breaks. This involves successive H atom migration and ring isomerization. The similar isomerization must occur in order to generate fragments C_6H_4 and NH_3. Since the minor channels observed in 4-methylpyridine correspond to the major channels in aniline and they have the similar translational energy distributions, some of the 4-methylpyridine must isomerize to aniline before dissociation occurs. A reasonable isomerization mechanism that explains the experimental results is the isomerization similar to that of toluene and xylene found in our previous experiments.[22,23] The isomerization starts from the change of 4-methylpyridine to a seven-membered ring isomer.

After the isomerization to the seven-membered ring isomer, the exchange of relative nitrogen and carbon atoms' positions occur through H migration around the seven-membered ring. In the end, the rearomatization of seven-membered ring to six-membered ring produces both methylpyridine and aniline. The subsequent dissociation produces all kinds of fragments we observed in the experiment.

$$C_5NH_4CH_3^{\ddagger} \rightarrow \text{c-}C_6NH_7^{\ddagger}$$
(6 to 7 membered ring isomerization) (4)

$$\text{c-}C_6NH_7^{\ddagger} \rightarrow \text{c-}C_6NH_7^{\ddagger}$$
(H atom migration in 7-membered ring) (5)

$$\text{c-}C_6NH_7^{\ddagger} \rightarrow C_5NH_4CH_3^{\ddagger}$$
(rearomatization to methylpyridine) (6a)

$$\text{c-}C_6NH_7^{\ddagger} \rightarrow C_6H_5NH_2^{\ddagger}$$ (rearomatization to aniline) (6b)

$$C_5NH_4CH_3^{\ddagger} \rightarrow C_5NH_4CH_2 + H$$
(dissociation after rearomatization) (7a)

$$C_5NH_4CH_3^{\ddagger} \rightarrow C_5NH_4 + CH_3$$
(dissociation after rearomatization) (7b)

$$C_6H_5NH_2^{\ddagger} \rightarrow C_6H_5 + NH_2$$
(dissociation after rearomatization) (7c)

$$C_6H_5NH_2^{\ddagger} \rightarrow C_6H_4 + NH_3$$
(dissociation after rearomatization) (7d)

$$C_6H_5NH_2^{\ddagger} \rightarrow C_6H_3NH_2 + H_2$$
(dissociation after rearomatization) (7e)

Although reaction 7e was not observed in 4-methylpyridine due to the obstacle of multiphoton dissociation, it is likely to occur since it is one of the major dissociation channels of aniline.

The observation of CD_3, CD_2H, CDH_2, and CH_3, from d_3-4-methylpyridine indicates some molecules undergo isotope exchange prior to dissociation. These exchanges can be achieved by the H and D atom migration around seven-membered ring in reaction 5. Fragment isotope ratios of $[CH_3 + CH_2D + CHD_2]/[CD_3]$ from d_3-4-methylpyridine suggest that 10% of 4-methylpyridine isomerize to seven-membered ring isomers and then rearomatize back to methylpyridine prior to dissociation.

(b) Aniline. Aniline is one of the aromatic molecules that the UV photochemistry has been studied extensively. High-resolution laser induced fluorescence spectroscopy of the S_1 state has been investigated, and the fluorescence lifetime and quantum yield of each vibronic level were obtained.[27] It shows that the fluorescence lifetime is about 5∼9 ns and quantum yield is 0.1∼0.2, depending on the vibronic levels. Intersystem crossing is the main nonradiative process in the S_1 state relaxation. The rate of intersystem crossing as large as 8.2×10^7 s^{-1} was found.[27] The decay of the triplet state generated from the S_1 state through intersystem crossing is very fast. Triplet state lifetime at the energy level corresponding to band origin of the S_1 state (294 nm) is 5653 ns, but it decreases rapidly as the energy increases. Lifetime as short as 168 ns was observed at energy 3800 cm^{-1} above the S_1 band origin.[28] Although the intersystem crossing rate from S_1 to T_1 is fast, however, no phosphorescence was observed in the gas phase due the rapid decay from T_1 to S_0.

Compared to the studies of the S_1 state, the photochemistry at 193 nm has received little attention. Early experimental investigation[29,30] and recent theoretical study[31] suggest the absorption of 193 nm photons corresponds to the excitation of electrons of the phenyl ring ($\pi-\pi^*$). Internal conversion of the phenyl ring electronic excited state at such high energy level usually is very fast. The dissociation therefore is expected to be very similar to that of 4-methylpyridine, i.e., dissociation occurs in the ground state and the channels with low dissociation barrier heights are the dominant processes. Indeed, cleavage through weak chemical bonds such as N−H and C−N bonds were found to be the major dissociation channels. Dissociation occurs in the ground electronic state is further confirmed by the fact that the maximum translational energy release of the H_2 elimination reaches the maximum available energy of the reaction $C_6H_5NH_2 \rightarrow C_6H_3NH_2 + H_2$. Since the fragment with maximum translational energy corresponds to the products $C_6H_3NH_2$ and H_2 produced in the ground electronic state and the ground state of these two close shell fragments only correlates to the ground state of the parent molecule, the dissociation must result in the ground electronic state.

The observation of fragment C_5NH_4 and CH_3 from aniline and various isotope-substituted fragments such as NH_3, NH_2D, NHD_2 from d_5-aniline can be explained by the similar isomerization and dissociation mechanism described in 4-methylpyridine, i.e., the isomerization from aniline to seven-membered ring, followed by H and D atom migration in seven-membered ring, and then the rearomatization to both aniline and methylpyridine prior to dissociation.

Although there are many similarities between the dissociation properties of 4-methylpyridine and aniline, however, some difference was also observed. For example, the elimination of close shell molecules, like H_2, NH_3, plays a very important role in aniline, but they were not observed in the direct dissociation of 4-methylpyridine. In addition, the fast component in the translational energy distributions of H atom elimination was only found in aniline. This component must result from the dissociation in the excited state of a repulsive potential, or from an electronic state with a large exit barrier. Since the reverse reaction of H atom elimination has no barrier in the ground electronic state, the fast component must result from the dissociation in the electronic excited state. Very recently, it was proposed that in several aromatic molecules, a $\pi\sigma^*$ state exists in the vicinity of S_1 state,[32−34] and the potential energy surface of this state is essentially a repulsive state along the N−H coordinate. It is possible that the fast component of H atom elimination we observed in the experiment resulted from this state. Since the fragment distribution of the fast component is isotropic, dissociation does not occur directly on the repulsive

(27) Scheps, R.; Florida, D.; Rice, S. A. *J. Chem. Phys.* **1974**, *61*, 1730−1747.
(28) Knee, J. L.; Johnson, P. M.; *J. Chem. Phys.* **1984**, *80*, 13−17.
(29) Kimura, K.; Tsubomura, H.; Nagakura, S.; *Bull. Chem. Soc. Jpn.* **1964**, *37*, 1336−1346.
(30) Kimura, K.; Nagakura, *Mol. Phys.* **1965**, *9*, 117-?.
(31) Honda, Y.; Hada, M.; Ehara, M.; Nakasuji, H. *J. Chem. Phys.* **2002**, *117*, 2045−2052.
(32) Sobolewski, A. L.; Domcke, W. *J. Phys. Chem. A.* **2001**, *105*, 9275−9283.
(33) Sobolewski, A. L.; Domcke, W.; Dedonder-Lardeux, C.; Jouvet, C. *Phys. Chem. Chem. Phys.* **2002**, *4*, 1093−1100.
(34) Ebata, T.; Minejima, C.; Mikami, N. *J. Phys. Chem. A.* **2002**, *106*, 11 070−11 074.

potential energy surface. Instead, dissociation must occur indirectly through the coupling between the repulsive surface and other excited states on a time scale much longer than the parent molecule rotation. On the other hand, H atom elimination also has an exit barrier in the triplet state. Dissociation from the triplet state cannot be totally excluded without the additional information about the intersystem crossing quantum yield at this wavelength.

The isomerization and dissociation mechanism of aniline can be summarized as followings.

$$C_6H_5NH_2 + h\nu_{193nm} \rightarrow C_6H_5NH_2^* \text{ (excitation)} \quad (8)$$

$$C_6H_5NH_2^* \rightarrow C_6H_5NH_2^{\ddagger} \text{ (internal conversion to } S_0) \quad (9)$$

$$C_6H_5NH_2^* \rightarrow C_6H_5NH + H \text{ (dissociation from excited state)} \quad (10)$$

$$C_6H_5NH_2^{\ddagger} \rightarrow C_6H_5NH + H \text{ (direct dissociation after internal conversion)} \quad (11a)$$

$$C_6H_5NH_2^{\ddagger} \rightarrow C_6NH_5 + H_2 \text{ (direct dissociation after internal conversion)} \quad (11b)$$

$$C_6H_5NH_2^{\ddagger} \rightarrow C_6H_5 + NH_2 \text{ (direct dissociation after internal conversion)} \quad (11c)$$

$$C_6H_5NH_2^{\ddagger} \rightarrow C_6H_4 + NH_3 \text{ (direct dissociation after internal conversion)} \quad (11d)$$

$$C_5NH_4CH_3^{\ddagger} \rightarrow c\text{-}C_6NH_7^{\ddagger} \text{ (6 to 7 membered ring isomerization)} \quad (12)$$

Reactions following reaction 12 are the same as reactions (5)∼-(7).

According to this isomerization and dissociation mechanisms, the ratio $[ND_3 + NHD_2]/[NH_2D]$ observed from d_5-aniline indicates that 23% of aniline in the ground electronic state isomerize to seven-membered ring, followed by H/D atom migration, and then rearomatize to aniline prior to dissociation.

Although the slow dissociation rates and translational energy distributions obtained from the experimental measurement suggest that both aniline and 4-methylpyridine dissociation occurs on the ground electronic state (except the fast component of H atom elimination in aniline), the possibility that isomerization occurs to some extent in the excited state before molecules reach the ground state through internal conversion cannot be totally excluded. This kind of isomerization, like pyridine undergoes ring opening isomerization in the excited state, has been observed.[35] However, the different intermediates produced directly in the electronic excited state from 4-methylpyridine and aniline, respectively, must be able to isomerize to each other with low enough barrier heights in order to explain the experimental results. Due to the lack of excited-state potential energy surfaces at this moment, there is no compelling evidence to claim their intermediacy in the present case.

B. Potential Energy Surface. This particular isomerization between six-membered ring and seven-membered ring is supported by ab initio calculations. The energies of isomers and various transition states along the isomerization and dissociation pathways from ab initio calculation are shown in Figure 10. In the calculation, the geometries were optimization by B3LYP/6-31G* and the energies were calculated by G3 scheme. The dissociation of 4-methylpyridine has barrier heights of 91.0 kcal/mol for C−H bond cleavage, and 105.9 kcal/mol for C−C bond cleavage. The isomerization of 4-methylpyridine to seven-membered ring starts with the H atom shift from methyl group to the carbon atom next to the methyl group, followed by the formation of bicyclo-isomer as an intermediate, and finally the isomerization to form seven-membered ring isomer. The six-membered ring to seven-membered ring isomerization has a barrier height of 88.7 kcal/mol. Since the barrier heights are all very close in energy, isomerization to seven-membered ring competes with C−C bond and C−H bond dissociation. Although most of the 4-methylpyridine molecules dissociate directly through C−C and C−H bond cleavages after the internal conversion, however, experimental data shows that at least 10% of 4-methylpyridine molecules isomerize to seven-membered ring prior to dissociation.

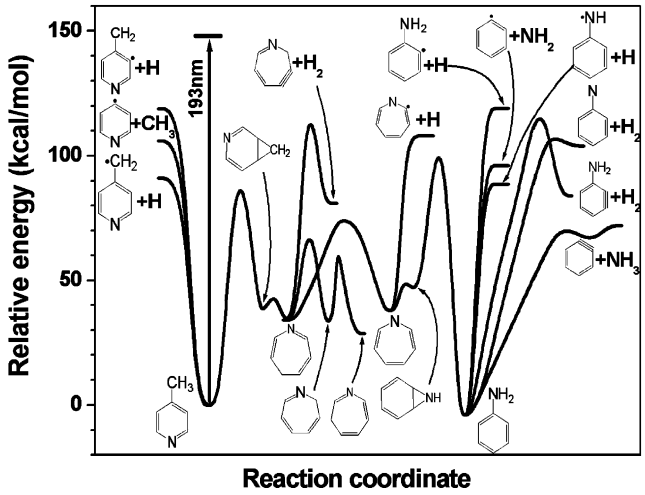

Figure 10. Energy diagram for isomerization and dissociation of 4-methylpyridine and aniline. The energies were computed at the G3 level of theory and the geometry optimized by B3LYP/6-31G*.

Dissociation and isomerization barrier heights in the ground electronic state of aniline show the similar properties to that of 4-methylpyridine. Eliminations of H atom, H_2, NH_2, NH_3 have barrier heights of 86.4, 104∼116, 100.7, and 72 kcal/mol, respectively. Isomerization of aniline to seven-membered ring isomer also starts with the H atom shift from amino group to the carbon atom next to the amino group, forming a bicyclo-intermediate, and then followed by the isomerization to seven-membered ring. The barrier height of the isomerization is only 102.4 kcal/mol, which is very close to various dissociation barrier heights. Isomerization to seven-membered ring therefore competes with the direct dissociation channels in the ground electronic state. Most of the aniline molecules in the ground electronic state dissociate directly, but at least 23% of aniline in the ground-state isomerize to seven-membered ring.

It is interesting to note that there are four different seven-membered ring isomers, depending on the positions of H atoms. Among these isomers, 1-aza-1,3,6-cycloheptatriene and 1-aza-2,4,6-cycolheptatriene can be produced directly from 4-methylpyridine and aniline respectively after the six-membered ring to seven-membered ring isomerization. The other isomers including 1-aza-2,4,7-cycloheptatriene and 1-aza-1,3,5-cyclo-

(35) Lobastov, V. A.; Srinivasan, R.; Goodson, B. M.; Ruan, C. Y.; Feenstra, J. S.; Zewail, A. H. *J. Phys. Chem. A.* **2001**, *105*, 11 159−11 164.

heptatriene require further H atom migration around the seven-membered ring. For example, 1-aza-1,3,5-cycloheptatriene can be produced from 1-aza-1,3,6-cycloheptatriene through 2,5-H shift, and 4,7-H shift of 1-aza-1,3,5-cycloheptatriene can generate 1-aza-2,4,7-cycloheptatriene. The isomerization between 1-aza-1,3,6-cycloheptatriene and 1-aza-2,4,6-cycolheptatriene can be achieved through 1,5-H shift. The barrier heights between these seven-membered ring isomers are only about 32∼40 kcal/mol. Consequently, H and D atoms can easily migrate around the seven-membered ring due to the low barrier heights, resulting in several seven-membered ring isomers. The exchange of H and D atom and the change of relative nitrogen and carbon atoms' positions all come from these H or D atom migration around the seven-membered ring.

The potential energies corresponding to the elimination of close shell molecules including H_2 and NH_3 are also shown in Figure 10. NH_3 elimination starts from the migration of H atom in the position 2 toward N atom of the amino group, followed by forming the $C_6H_4-NH_3$ complex, and then NH_3 elimination occurs. It has the lowest dissociation threshold. The maximum available energy is as large as 75 kcal/mol. As a result, the photofragment translational energy release in this channel is relatively large.

In contrast to NH_3 elimination, there are many dissociation channels leading to H_2 elimination. They can be classified into two types of H_2 elimination, according to the values of the exit barrier height. The H atoms can be both eliminated from phenyl ring and produce 2-aminobenzyne and 3-aminobenzyne. The calculation shows that they are endothermic by 80.6 and 83.8 kcal/mol and have the dissociation barriers of 113.4 and 119.3 kcal/mol, respectively. The exit barrier heights for this type of elimination channel are as large as 32.8 and 35.5 kcal/mol, respectively. This type of H_2 elimination occurs through the H atom migration in phenyl ring, and then H_2 dissociated from the parent molecule through three-center elimination. It is similar to the benzene H_2 elimination mechanism.[36] Another channel belonging to this type of elimination is the H_2 elimination from seven-membered ring. The barrier height is 114.6 kcal/mol, and it is endothermic by 81 kcal/mol. The exit barrier of 33 kcal/mol in this channel is similar to the values in the other two channels. For the other type of H_2 elimination, H atoms can be both eliminated from amino group, or one is from amino group and the other is from phenyl ring. This type of H_2 elimination has dissociation barriers of 104.2 and 110 kcal/mol and is endothermic by 103.1 and 105.7, respectively. In contrast to the other type of H_2 elimination, the exit barriers are small. They are only 1.1 and 4.3 kcal/mol.

The photofragment translational energy distribution of the H_2 elimination shows two components, indicating two different dissociation mechanisms. For the fast component, the average released translational energy is large, and the peak of the distribution is located at 23 kcal/mol. It must result from a dissociation channel with large exit barrier, i.e., both H atoms are eliminated from phenyl ring and benzyne-like derivatives are produced, or from the seven-membered ring isomer. This can be confirmed from the fact that the maximum translational energy of the fast component reaches the maximum available energies of these reaction $C_6H_5NH_2 \rightarrow C_6H_3NH_2$ (or c-C_6NH_5 within experimental error) + H_2, corresponding to the products $C_6H_3NH_2$ (or c-C_6NH_5) and H_2 produced in the ground electronic state. On the other hand, the slow component has limited translational energy released. It must result from a dissociation channels with small exit barrier, corresponding to both H atoms eliminated from amino group or one from amino group and the other from phenyl ring. However, this type of H_2 elimination is less than 10% of the total H_2 elimination.

C. Comparison to Photodissociation of Toluene. Toluene has the similar structure to those of methylpyridine and aniline. Since the photophysics and photochemistry processes of toluene have been studied extensively, it is thus interesting to compare the photodissociation of methylpyridine and aniline to that of toluene. Toluene in the S_2 state produced by 200 nm excitation was found to undergo fast internal conversion to the S_0 and S_1 states with a lifetime of ∼50 fs.[20] Dissociation rate of toluene after 193 nm excitation under collision-free conditions was found to be 2×10^6 s^{-1}.[22] The fast relaxation from the S_2 and S_1 states to S_0, and the slow dissociation rate suggest the dissociation occurs from the vibrationally excited ground electronic state after internal conversion. In the ground state, 75% of hot toluene dissociate directly through methyl H atom and CH_3 elimination. However, 25% of toluene isomerize to seven-membered ring and rearomatize back to toluene, and eventually they all dissociate through H and CH_3 elimination channels from six-membered ring. No dissociation from seven-membered ring isomer was observed.

4-methylpyridine has very similar dissociation properties to those of toluene. Most of the 4-methylpyridine dissociates through methyl C−H and C−CH_3 bond cleavages after internal conversion. Since seven-membered ring can isomerize to both methylpyridine and aniline, the ratio of [CH_3 + CH_2D + CHD_2]/[CD_3] from d_3-4-methylpyridine suggest that more than 10% of 4-methylpyridine molecules isomerize to seven-membered ring and then rearomatize to six-membered ring prior to dissociation. On the other hand, aniline shows different dissociation properties from those of toluene. Excited-state dissociation plays an important role at this photon energy. 75% of H elimination occurs in the electronic excited state. Although the NH_2 and H atom eliminations from the ground state and the isomerization to seven-membered ring are analogous to those of toluene, however, the elimination of closed shell molecules, like H_2 and NH_3 in aniline, were not observed in toluene. Indeed, closed shell molecule elimination channel has not been observed for any alkylbenzenes in this photon energy region.

Compared to 25% of toluene, at least 10% of 4-methylpyridine and more than 23% of aniline in the ground state isomerize to seven-membered ring and then rearomatize to six-membered ring prior to dissociation. The results demonstrate that this isomerization not only plays a very important role in toluene and xylene, but also plays a very important role in nitrogen atom contained aromatic molecules. The significance of this isomerization is that the carbon, nitrogen, and hydrogen atoms belonging to the alkyl or amino group are involved in an exchange with those atoms in the aromatic ring during the isomerization. They cannot be achieved by the other isomerization.

Acknowledgment. The work was supported by the National Science Council Taiwan, under contract NSC 92-2113-M-001-015.

JA0483894

(36) Mebel, A. M.; Lin, M. C.; Chakraborty, D.; Park, J.; Lin, S. H.; Lee, Y. T. *J. Chem. Phys.* **2001**, *114*, 8421−8435.